

# Damping Allocation in Automotive Structures using Reduced Models

Nicolas Roy <sup>1</sup> Sylvain Germès <sup>2</sup> Benjamin Lefebvre <sup>3</sup> Etienne Balmès <sup>4</sup>

1 Top Modal, 5 rue de la ZA de Ribaute, 31130 Quint-Fonsegrives, France  
email : [nicolas.roy@topmodal.fr](mailto:nicolas.roy@topmodal.fr)

2 PSA Peugeot Citroën, Dept. of Sciences for Automobiles and Advanced Research, 78943 Vélizy-Villacoublay  
email : [sylvain.germes@mpsa.com](mailto:sylvain.germes@mpsa.com)

3 PSA Peugeot Citroën, 78943 Vélizy-Villacoublay and Ecole Centrale Paris, 92295 Chatenay Malabry  
email : [benjamin.lefebvre@mpsa.com](mailto:benjamin.lefebvre@mpsa.com)

4 SDTools, 44 rue Vergniaud, 75013 Paris, France and Ecole Centrale Paris, 92295 Chatenay Malabry  
email : [balmes@sdtools.com](mailto:balmes@sdtools.com)

## Abstract

The use of passive damping has shown to be very effective in reducing low frequency mechanical vibrations in passenger vehicles. It is therefore necessary to account for damping at the design level by the introduction of damping specifications related to the vehicle's structural components or substructures.

This paper describes an ongoing development at PSA of a methodology and software tool for assessing and optimizing the allocation of damping in complex industrial structures. The tool makes extensive use of substructuring and mode superposition techniques offering computational efficiency and physical insight in order to quickly determine and understand the influence of the components on system behavior.

## 1 Introduction

Designing cars which meet stringent acoustic and vibration quality (ACV) specifications is becoming more and more difficult due to ever increasing customer demands and expectations.

Vehicle comfort is one of the buyer's most important criteria. Indeed, it accounts for more than one quarter of the customer's dissatisfaction. Comfort can be quantified in terms of mechanical vibrations (steering wheel, rear-view mirror, dashboard, etc.) and acoustic transmission (engine noise, wheels, etc.).

To satisfy design goals, stiffness modifications are typically introduced in areas where vibration levels are exceeded.

Unfortunately, the stiffened structure is obtained at the cost of added mass as illustrated in Figure 1. The approach also penalizes fuel consumption and increases pollution emission. Today, improved ACV specifications must take advantage of a new design parameter: damping.

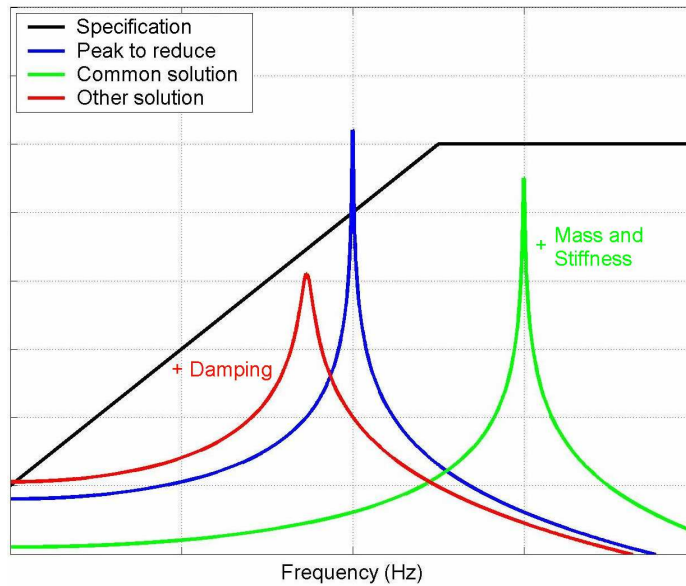


**Figure 1: Damping versus Mass and Stiffness**

In order to use this new design parameter in the automotive industry, the ACV teams are in charge of the specification of damping characteristics of each automobile part contributing to the noise environment inside the car.

The design process is presented in Figure 2. First, the specification phase focuses on obtaining a good vibroacoustic synthesis. This is followed by the design phase which involves the realization of the damping solutions.

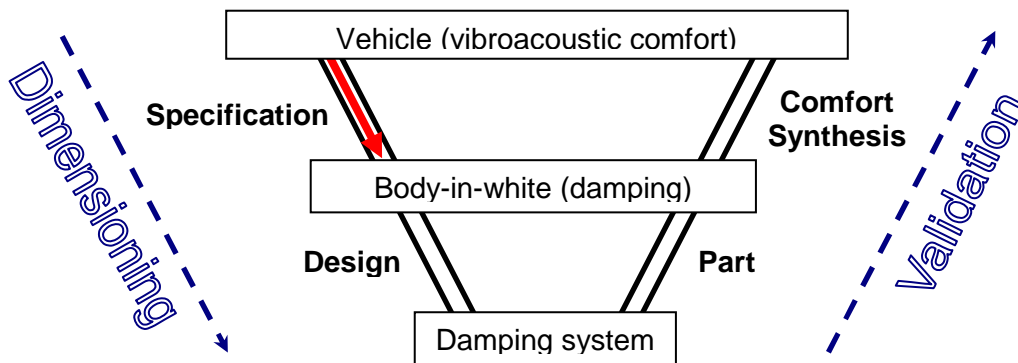


**Figure 2: Design Process**

This process requires, on one hand, the development of suitable methods and software tools for the damping specification of the different parts (body, equipment, etc.), and on the other hand, the design of damping systems which satisfy these specifications.

This article describes the specification phase of the design process. First, the theoretical aspects are presented including the use and interest of substructuring and energy criteria based on modal participation factors. Next the methodology is outlined followed by an industrial application.

## 2 Theoretical Background

### 2.1 Reduced Models

Consider a substructure,  $S$ , depicted in Figure 3, with  $g$  total degrees of freedom (DOFs). Of particular interest among the  $g$  DOFs are the connection (interface) DOFs,  $c$ , the excitation DOFs,  $e$ , and the observation (response) DOFs,  $o$ .

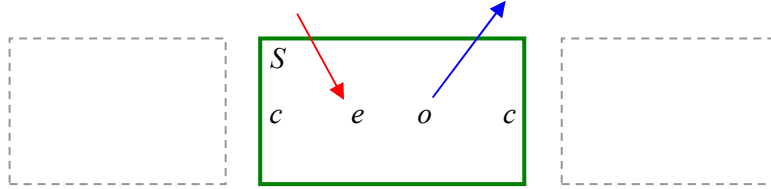


Figure 3: Substructure,  $S$ , and Degrees of Freedom

A transformation may be defined using a suitable basis of modes for the substructure comprising  $k$  free-interface normal modes,  $\Phi_{gk}^S$ , and  $s$  residual flexibilities,  $\mathbf{G}_{gs}^S$ , where  $s = c + e$ .

$$\mathbf{u}_g^S = \begin{bmatrix} \Phi_{gk}^S & \mathbf{G}_{gs}^S \end{bmatrix} \begin{bmatrix} \mathbf{q}_k^S \\ \mathbf{f}_s^S \end{bmatrix} \quad (1)$$

The normal modes of the substructure are obtained by solving the following eigenvalue problem using the substructure's global stiffness and mass matrices,  $\mathbf{K}_{gg}^S$  and  $\mathbf{M}_{gg}^S$ .

$$\left( \mathbf{K}_{gg}^S - \omega_k^2 \mathbf{M}_{gg}^S \right) \Phi_{gk}^S = 0 \quad (2)$$

The residual flexibilities are obtained by applying unit forces at each of the  $s$  DOF and then removing the modal contribution from the resulting flexibilities. This can be performed in a single step by the use of Lagrange multipliers as shown in Equation (3).

$$\begin{bmatrix} \mathbf{K}_{gg}^S & \mathbf{M}_{gg}^S \Phi_{gk}^S \\ \Phi_{kg}^S & \mathbf{M}_{gg}^S \end{bmatrix} \begin{bmatrix} \mathbf{G}_{gs}^S \\ \lambda_{ks} \end{bmatrix} = \begin{bmatrix} \mathbf{I}_{gs} \\ \mathbf{0}_{ks} \end{bmatrix} \quad (3)$$

Although the basis of Equation (1) can be used directly, it is preferable to convert the residual flexibilities to residual modes in order to simplify implementation. The advantage of residual modes is that they are orthogonal to each other (as well as to the normal modes) and can therefore be "treated" as a set of additional normal modes.

Details and applications concerning residual modes and enriched modal bases may be found in several publications including [1, 2, 3].

Replacing the residual flexibilities in Equation (1) by equivalent residual modes,  $\hat{\Phi}_{gs}^S$ , leads to the following simplified transformation with  $b = k + s$ .

$$\mathbf{u}_g^S = \Phi_{gb}^S \mathbf{q}_b^S = \begin{bmatrix} \Phi_{gk}^S & \hat{\Phi}_{gs}^S \end{bmatrix} \begin{bmatrix} \mathbf{q}_k^S \\ \mathbf{q}_s^S \end{bmatrix} \quad (4)$$

Using the above transformation, the substructure's mass and stiffness matrices may then be condensed to obtain the generalized masses and stiffnesses,  $\mathbf{m}_b^S$  and  $\mathbf{k}_b^S$ .

$$\mathbf{m}_b^S = \Phi_{bg}^S \mathbf{M}_{gg}^S \Phi_{gb}^S \quad \mathbf{k}_b^S = \Phi_{bg}^S \mathbf{K}_{gg}^S \Phi_{gb}^S \quad (5)$$

Using Equations (4) and (5), a reduced model can be elaborated as illustrated in Figure 4. The  $b$  modes of the basis are represented by scalar spring-mass systems. Structural damping associated with the substructure,  $\eta^S$ , is introduced as an imaginary component of the spring stiffness. Linear constraint equations are used to recover the physical displacements at the connection, excitation and observation DOFs. Stiff springs,  $\mathbf{k}_s^S$ , are included in the reduced model to render the connection and excitation DOFs independent thus facilitating substructure assembly. The reduced model of Figure 4 can be easily elaborated as a finite element model using standard features.

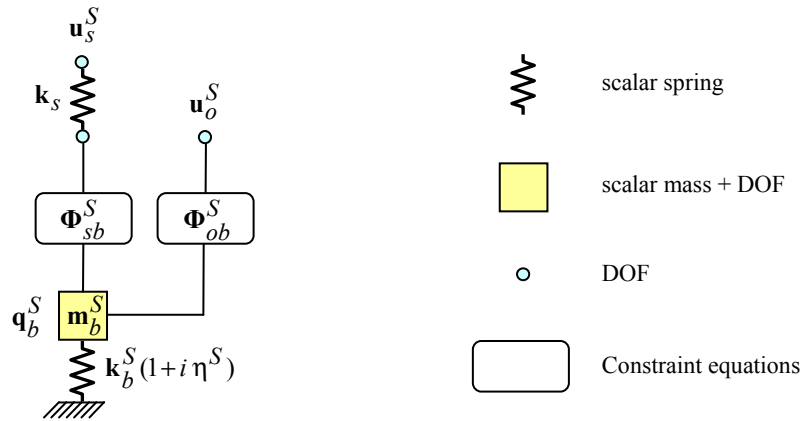


Figure 4: Reduced Model of Substructure  $S$

## 2.2 Modal Participation Factors

Following reduction of each substructure, the resulting reduced models may be directly assembled to form the global structure illustrated in Figure 5.

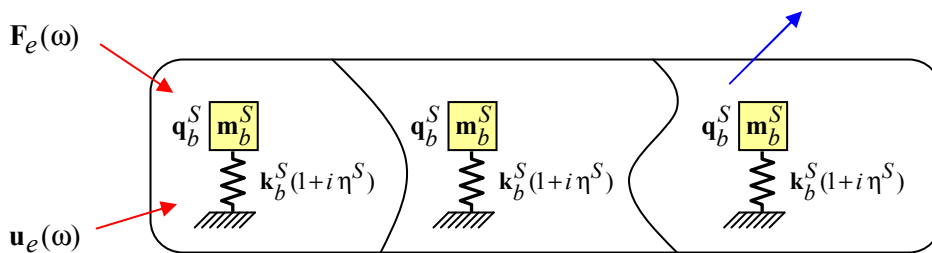


Figure 5: Global Structure from Assembly of Reduced Models

For a given harmonic excitation (applied force,  $\mathbf{F}_e(\omega)$  or imposed displacement  $\mathbf{u}_e(\omega)$ ), the equations of motion of the global structure may be readily solved for the physical responses,  $\mathbf{u}_o(\omega)$ .

In addition, the generalized responses,  $\mathbf{q}_b^S(\omega)$ , which are calculated as well, may be used to quantify the contribution of the substructure modes to the physical response via modal participation factors (MPF) defined hereafter.

We start by defining the modal strain energies,  $\mathbf{E}_b^S(\omega)$ , associated with the generalized responses,  $\mathbf{q}_b^S(\omega)$ .

$$\mathbf{E}_b^S(\omega) = \frac{1}{2} \left| \mathbf{q}_b^S(\omega) \right|^2 \mathbf{k}_b^S \quad (6)$$

Equation (6) is analogous to the expression used by finite element codes to calculate the mean strain energy within a given element,  $e$ , where  $u_r$  and  $u_i$  are the real and imaginary parts of the response, and  $K_e$  the element stiffness matrix.

$$\mathbf{E}_e = \frac{1}{4} \left( \{u_r\}^T [K_e] \{u_r\} + \{u_i\}^T [K_e] \{u_i\} \right) \quad (7)$$

Unlike the generalized responses,  $\mathbf{q}_b^S(\omega)$ , which are complex valued and depend on the mode shape normalization, the strain energies,  $\mathbf{E}_b^S(\omega)$ , are real valued and independent of the normalization. The MPF are defined by dividing the strain energies by the total energy over all modes and substructures.

$$\mathbf{MPF}_b^S(\omega) = \frac{\mathbf{E}_b^S(\omega)}{\sum_S \sum_b \mathbf{E}_b^S(\omega)} \quad (8)$$

Each MPF indicates the fraction of energy in a given mode,  $b$ , of a given substructure,  $S$ . By summing the MPF over each substructure's modes, we can quantify the energy contribution per substructure.

$$\mathbf{MPF}^S(\omega) = \sum_b \mathbf{MPF}_b^S(\omega) \quad (9)$$

By definition, the MPF respect the following summation rules.

$$0 \leq \mathbf{MPF}_b^S(\omega) \leq 1 \quad \text{and} \quad \sum_S \sum_b \mathbf{MPF}_b^S(\omega) = \sum_b \mathbf{MPF}^S(\omega) = 1 \quad (10)$$

Finally, the modal contributions to the physical response,  $\mathbf{u}_o(\omega)$ , may be simply obtained by multiplying the response by the MPF leading to:

$$\mathbf{u}_{o,b}^S(\omega) = \mathbf{u}_o(\omega) \times \mathbf{MPF}_b^S(\omega) \quad (11)$$

$$\mathbf{u}_o^S(\omega) = \mathbf{u}_o(\omega) \times \mathbf{MPF}^S(\omega) \quad (12)$$

## 2.3 Damping Allocation and Response Attenuation

A global structural damping value,  $\eta(\omega)$ , can be defined from the MPF and the substructure damping values,  $\eta^S$ .

$$\eta(\omega) = \sum_S \left( \eta^S \times \mathbf{MPF}^S(\omega) \right) \quad (13)$$

If we assume that the amplitude of a given response,  $|\mathbf{u}_o(\omega)|$ , is inversely proportional to the global damping, this leads to the following expression.

$$\frac{|\mathbf{u}_o(\omega) + \Delta\mathbf{u}_o(\omega)|}{|\mathbf{u}_o(\omega)|} = \frac{\eta(\omega)}{\eta(\omega) + \Delta\eta(\omega)} \quad (14)$$

In reality, Equation (14) is approximate since coupling between modes is ignored. Nonetheless, in the vicinity of isolated peaks, Equation (14) can be used to provide a quick and relatively accurate estimation of response attenuation,  $A(\omega)$ , for a given damping allocation.

$$A(\omega) = \frac{\eta(\omega)}{\eta(\omega) + \Delta\eta(\omega)} \quad (15)$$

$$\text{where} \quad \Delta\eta(\omega) = \sum_S \Delta\eta^S \times \mathbf{MPF}^S(\omega) \quad (16)$$

The estimation of the attenuated response is obtained by multiplying the response by the attenuation.

$$\mathbf{u}_o(\omega) + \Delta\mathbf{u}_o(\omega) = A(\omega) \times \mathbf{u}_o(\omega) \quad (17)$$

Note that values of  $A > 1$  indicate an amplification rather than an attenuation.

In practice, we would like to allocate damping in order to satisfy a given level of attenuation. This is equivalent to satisfying the following expression obtained by substituting Equation (16) into Equation (15)

$$\sum_S \Delta\eta^S \times \mathbf{MPF}^S(\omega) = \left( \frac{1}{A(\omega)} - 1 \right) \eta(\omega) \quad (18)$$

while imposing variation limits on  $\Delta\eta^S$ :

$$0 \leq \Delta\eta^S \leq \Delta\eta_{\max}^S \quad (19)$$

Equations (18) and (19) can be solved using one of several classic optimization algorithms such as Non-Negative Least Squares (NNLS). Note that depending on the particular system to be optimized, there may be a unique solution, an infinite number of solutions or no solution (i.e. sub-optimal solution).

### 3 Methodology

#### • Introduction

The substructure approach to damping specification has been implemented using MATLAB® and MSC/NASTRAN® within a methodology comprising 4 principal steps listed in Figure 6 and described hereafter.

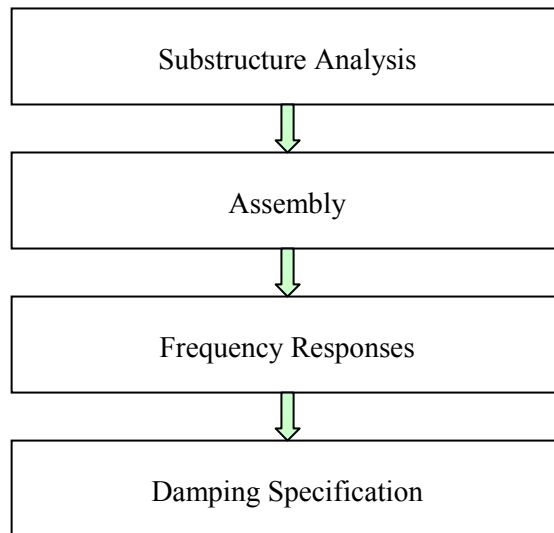


**Figure 6: Principal Steps of Methodology**

#### • Substructure Analysis

The first step involves the definition and preparation of the structural components comprising the system to be analyzed. Each component should correspond to a physical part of the structure associated with a particular damping level or capacity to dissipate energy.

For each substructure, the connection, excitation and observation DOFs are specified in the NASTRAN input file.

A modal analysis is performed for each substructure in order to compute the normal and residual modes needed to elaborate the reduced model. The frequency range of the normal modes depends on the particular study and should extend to at least 1.5 times the highest excitation frequency in order to minimize modal truncation errors. This step is performed within NASTRAN.

#### • Assembly

Following substructure analysis, the reduced models are created as NASTRAN spring-mass models using the schema shown in Figure 4, and then assembled by introducing displacement compatibility constraints at the connection DOFs. This step is performed entirely within MATLAB.

#### • Frequency Responses

Frequency responses are defined via load cases in MATLAB. The following properties are configured for each load case:

- Excitation frequencies
- Excitation and response points
- Excitation level or profile
- Structural damping for each substructure

Once the load case has been defined, the corresponding frequency response calculation is exported to NASTRAN. Upon completion, the responses along with the modal participation factors (MPF) are imported to MATLAB for visualization and analysis.

### • Damping Specification

The computed frequency responses are plotted and compared to specification levels. At critical frequencies where response levels exceed allowable limits, the MPF are used to identify the substructure(s) contributing significantly to the total response. For these substructures, the MPF may be further used to identify the contributing substructure modes.

At the peaks exceeding the allowable levels, substructure damping values may be manually or automatically modified (optimized) to satisfy the desired attenuation. An estimation of the response with the new damping specification may be computed using the MPF. The exact attenuated response may be obtained by defining a new load case using the modified damping values.

## 4 Industrial Application

The damping allocation software tool and methodology are currently undergoing validation at PSA. One of the first industrial validation cases studied was a floorboard structure with 4 soundproof treated panels illustrated in Figure 7.

To assess and optimize the effectiveness of the damped panels, each panel was modeled as a separate substructure, with all remaining floorboard parts grouped into a single substructure.

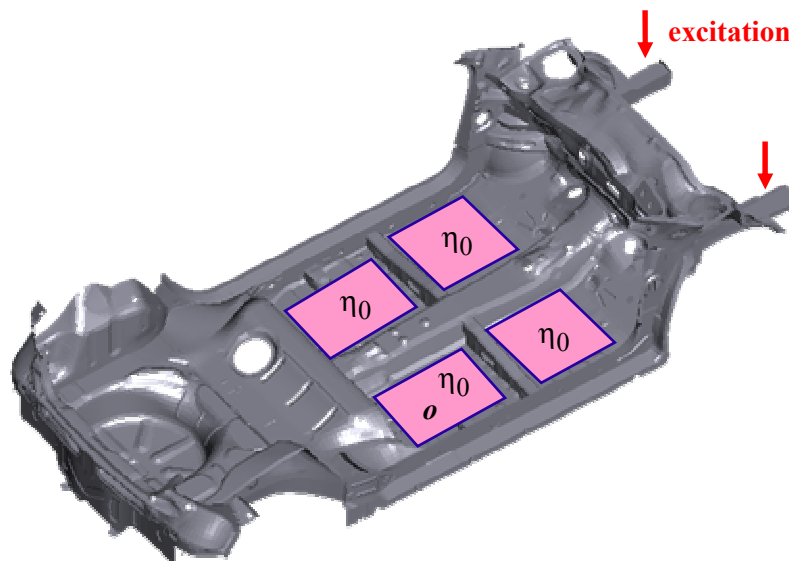


**Figure 7: Floorboard with 4 Damped Panels**



The floorboard structure was excited at the end of the cant rails as shown in Figure 7. The response was computed at the center of the damped panel indicated by "o". Nominal initial values of structural damping,  $\eta_0$ , were assigned to the 4 panels and floorboard substructure.

The initial response is plotted in Figure 8 along with the specification level. There are 3 peaks that exceed the specification level. MPF analysis of the first peak (a), indicated negligible contribution of the panel substructure. This is confirmed by visualization of the corresponding mode shape which is a global deformation of the floorboard. Therefore damping allocation will be ineffective for this peak.

With regards to the second peak (b), the MPF values revealed a significant contribution coming from the panel component. This is confirmed by the corresponding mode shape which is a local panel mode. Attenuation of this peak by damping specification is therefore possible.

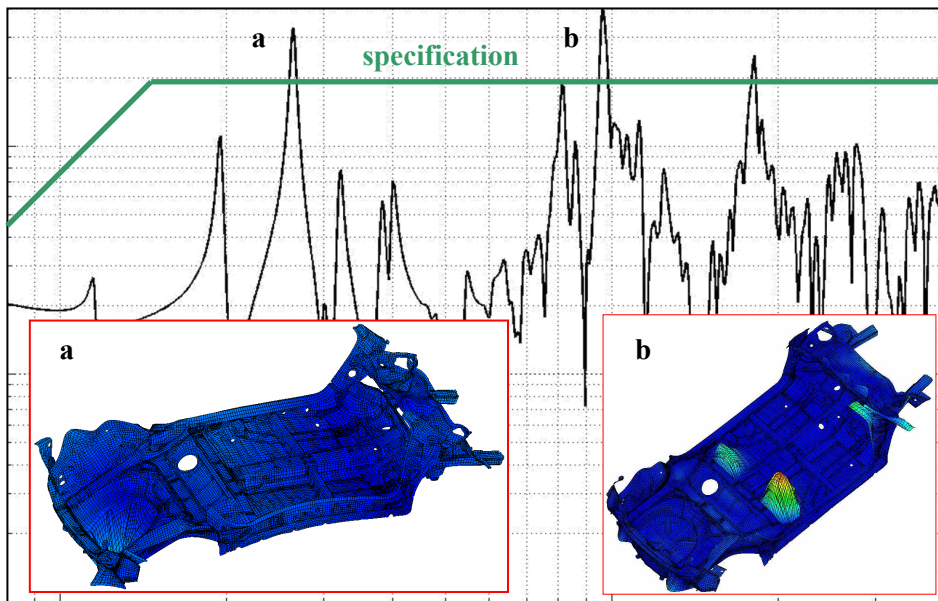


**Figure 8: Initial Frequency Response with Specification Level**

In order to satisfy specifications for the peak (b), damping specification was optimized for the 4 damped panels. The new damping values are indicated in Figure 9 and expressed with respect to the initial damping,  $\eta_0$ .

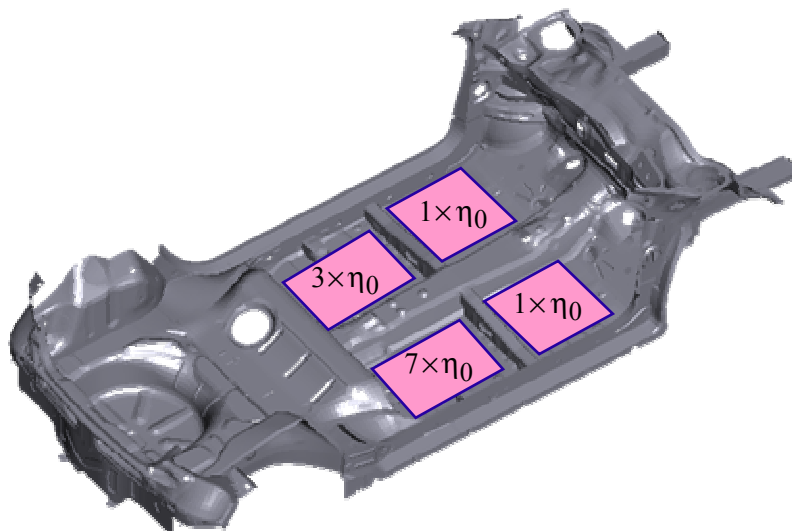


**Figure 9: Optimized Damping Specification**

Finally, the frequency response using the specified damping values is plotted in Figure 10 (magenta) on top of the initial response (black). As expected, in the low frequency range, the panel damping has little effect on the response level. On the other hand, the mid-frequency peak at (b) has been effectively attenuated to the specification level. The third peak that exceeded the specification has also been significantly attenuated.

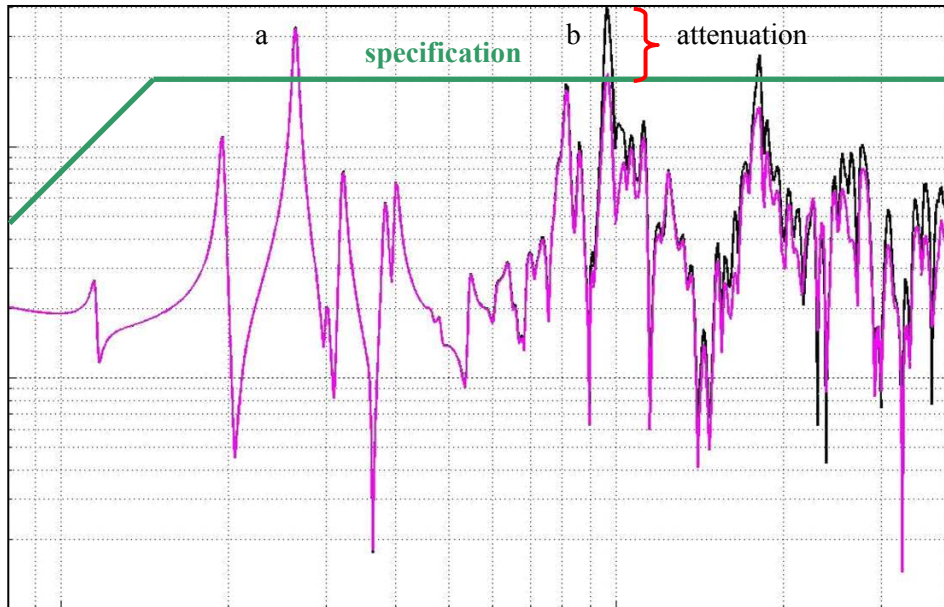


**Figure 10: Final Response (magenta) with Initial Response (black)**

## 5 Conclusions

A methodology and software tool for optimal damping specification has been developed at PSA to provide an effective alternative to stiffness and mass approaches used during preliminary design of a vehicle. The feasibility and interest of the methodology has been demonstrated on a industrial structure involving a floorboard equipped with damped panels. Ongoing work includes continued validation, improvements to numerical algorithms and enhancements such as vibroacoustic coupling.

## References

- [1] N. Merlette, S. Germès et al, *The Use of Suitable Modal Bases for Dynamic Prediction of Structures Containing High Damping Materials*, ISMA, Leuven, 2004.
- [2] A. Bobillot, E. Balmès, *Iterative Techniques for Eigenvalue Solutions of Damped Structures Coupled with Fluids*, 43<sup>rd</sup> AIAA/ASME/ASCI/AHS/ASC Structures, Structural Dynamics and Materials Conference, Denver, 2002.
- [3] N. Roy, A. Girard, *Impact of Residual Modes in Structural Dynamics*, Proceedings, European Conference on Spacecraft Structures, Materials & Mechanical Testing, Noordwijk, The Netherlands, 2005.